

Neutrinoless Double Beta Decay Searches

Aksel Hallin
Victoria, BC
May, 2019

Neutrino Oscillations

$$\begin{pmatrix} \nu_e \\ \nu_\mu \\ \nu_\tau \end{pmatrix} = U_{\text{PMNS}} \begin{pmatrix} \nu_1 \\ \nu_2 \\ \nu_3 \end{pmatrix}$$

$$U_{\text{PMNS}} = \begin{pmatrix} 1 & 0 & 0 \\ 0 & c_{23} & s_{23} \\ 0 & -s_{23} & c_{23} \end{pmatrix} \begin{pmatrix} c_{13} & 0 & s_{13}e^{-i\delta_{\text{CP}}} \\ 0 & 1 & 0 \\ -s_{13}e^{i\delta_{\text{CP}}} & 0 & c_{13} \end{pmatrix} \begin{pmatrix} c_{12} & s_{12} & 0 \\ -s_{12} & c_{12} & 0 \\ 0 & 0 & 1 \end{pmatrix} \begin{pmatrix} e^{i\alpha_1} & 0 & 0 \\ 0 & e^{i\alpha_2} & 0 \\ 0 & 0 & 1 \end{pmatrix}$$

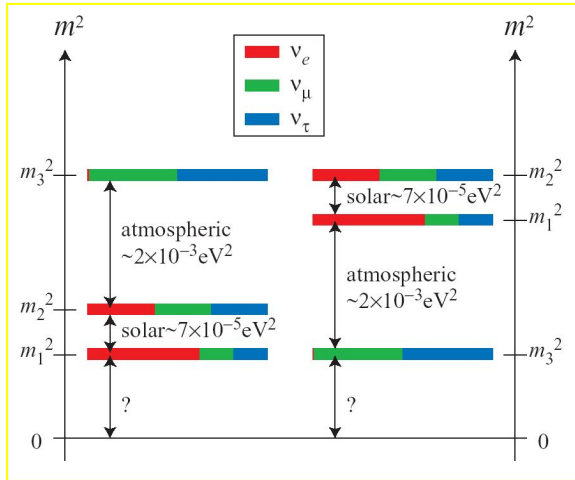
Pontecorvo-Maki-Nakagawa-Sakata Matrix

	Normal Ordering (best fit)		Inverted Ordering ($\Delta\chi^2 = 4.7$)		
	bfp $\pm 1\sigma$	3σ range	bfp $\pm 1\sigma$	3σ range	
	without SK atmospheric data				
$\sin^2 \theta_{12}$	$0.310^{+0.013}_{-0.012}$	0.275 \rightarrow 0.350	$0.310^{+0.013}_{-0.012}$	0.275 \rightarrow 0.350	
$\theta_{12}/^\circ$	$33.82^{+0.78}_{-0.76}$	31.61 \rightarrow 36.27	$33.82^{+0.78}_{-0.76}$	31.61 \rightarrow 36.27	
$\sin^2 \theta_{23}$	$0.580^{+0.017}_{-0.021}$	0.418 \rightarrow 0.627	$0.584^{+0.016}_{-0.020}$	0.423 \rightarrow 0.629	
$\theta_{23}/^\circ$	$49.6^{+1.0}_{-1.2}$	40.3 \rightarrow 52.4	$49.8^{+1.0}_{-1.1}$	40.6 \rightarrow 52.5	
$\sin^2 \theta_{13}$	$0.02241^{+0.00065}_{-0.00065}$	0.02045 \rightarrow 0.02439	$0.02264^{+0.00066}_{-0.00066}$	0.02068 \rightarrow 0.02463	
$\theta_{13}/^\circ$	$8.61^{+0.13}_{-0.13}$	8.22 \rightarrow 8.99	$8.65^{+0.13}_{-0.13}$	8.27 \rightarrow 9.03	
$\delta_{CP}/^\circ$	215^{+40}_{-29}	125 \rightarrow 392	284^{+27}_{-29}	196 \rightarrow 360	
$\frac{\Delta m_{21}^2}{10^{-5} \text{ eV}^2}$	$7.39^{+0.21}_{-0.20}$	6.79 \rightarrow 8.01	$7.39^{+0.21}_{-0.20}$	6.79 \rightarrow 8.01	
$\frac{\Delta m_{3\ell}^2}{10^{-3} \text{ eV}^2}$	$+2.525^{+0.033}_{-0.032}$	$+2.427 \rightarrow +2.625$	$-2.512^{+0.034}_{-0.032}$	$-2.611 \rightarrow -2.412$	
with SK atmospheric data	Normal Ordering (best fit)		Inverted Ordering ($\Delta\chi^2 = 9.3$)		
	bfp $\pm 1\sigma$	3σ range	bfp $\pm 1\sigma$	3σ range	
	$\sin^2 \theta_{12}$	$0.310^{+0.013}_{-0.012}$	0.275 \rightarrow 0.350	$0.310^{+0.013}_{-0.012}$	0.275 \rightarrow 0.350
	$\theta_{12}/^\circ$	$33.82^{+0.78}_{-0.76}$	31.61 \rightarrow 36.27	$33.82^{+0.78}_{-0.75}$	31.62 \rightarrow 36.27
	$\sin^2 \theta_{23}$	$0.582^{+0.015}_{-0.019}$	0.428 \rightarrow 0.624	$0.582^{+0.015}_{-0.018}$	0.433 \rightarrow 0.623
	$\theta_{23}/^\circ$	$49.7^{+0.9}_{-1.1}$	40.9 \rightarrow 52.2	$49.7^{+0.9}_{-1.0}$	41.2 \rightarrow 52.1
	$\sin^2 \theta_{13}$	$0.02240^{+0.00065}_{-0.00066}$	0.02044 \rightarrow 0.02437	$0.02263^{+0.00065}_{-0.00066}$	0.02067 \rightarrow 0.02461
	$\theta_{13}/^\circ$	$8.61^{+0.12}_{-0.13}$	8.22 \rightarrow 8.98	$8.65^{+0.12}_{-0.13}$	8.27 \rightarrow 9.03
	$\delta_{CP}/^\circ$	217^{+40}_{-28}	135 \rightarrow 366	280^{+25}_{-28}	196 \rightarrow 351
	$\frac{\Delta m_{21}^2}{10^{-5} \text{ eV}^2}$	$7.39^{+0.21}_{-0.20}$	6.79 \rightarrow 8.01	$7.39^{+0.21}_{-0.20}$	6.79 \rightarrow 8.01
$\frac{\Delta m_{3\ell}^2}{10^{-3} \text{ eV}^2}$	$+2.525^{+0.033}_{-0.031}$	$+2.431 \rightarrow +2.622$	$-2.512^{+0.034}_{-0.031}$	$-2.606 \rightarrow -2.413$	

$$U_{\text{PMNS}} = \begin{pmatrix} 1 & 0 & 0 \\ 0 & c_{23} & s_{23} \\ 0 & -s_{23} & c_{23} \end{pmatrix} \begin{pmatrix} c_{13} & 0 & s_{13} e^{-i\delta_{CP}} \\ 0 & 1 & 0 \\ -s_{13} e^{i\delta_{CP}} & 0 & c_{13} \end{pmatrix} \begin{pmatrix} c_{12} & s_{12} & 0 \\ -s_{12} & c_{12} & 0 \\ 0 & 0 & 1 \end{pmatrix} \begin{pmatrix} e^{i\alpha_1} & 0 & 0 \\ 0 & e^{i\alpha_2} & 0 \\ 0 & 0 & 1 \end{pmatrix}$$

Table 1. Three-flavour oscillation parameters from our fit to global data. The numbers in the 1st (2nd) column are obtained assuming NO (IO), i.e., relative to the respective local minimum. Note that $\Delta m_{3\ell}^2 \equiv \Delta m_{31}^2 > 0$ for NO and $\Delta m_{3\ell}^2 \equiv \Delta m_{32}^2 < 0$ for IO. The results shown in the upper (lower) table are without (with) adding the tabulated SK-atm $\Delta\chi^2$.

What we don't know



Absolute masses

Value δ_{CP} ?

CP Violation in Neutrino Sector?

Leptogenesis & Matter-Antimatter
Asymmetry in the Universe?

Are Neutrinos their own
Antiparticles?

Neutrinoless double beta decay provides input to several of these questions...

Double Beta Decay:

SEPTEMBER 15, 1935

PHYSICAL REVIEW

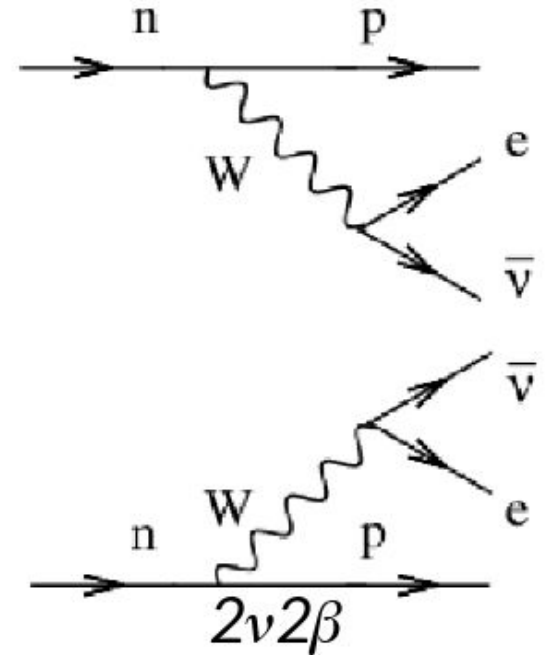
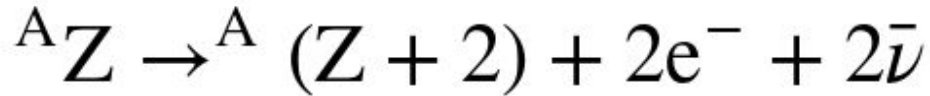
VOLUME 48

Double Beta-Disintegration

M. GOEPPERT-MAYER, *The Johns Hopkins University*

(Received May 20, 1935)

From the Fermi theory of β -disintegration the probability of simultaneous emission of two electrons (and two neutrinos) has been calculated. The result is that this process occurs sufficiently rarely to allow a half-life of over 10^{17} years for a nucleus, even if its isobar of atomic number different by 2 were more stable by 20 times the electron mass.



Neutrinoless Double Beta-Decay

DECEMBER 15, 1939

PHYSICAL REVIEW

VOLUME 56

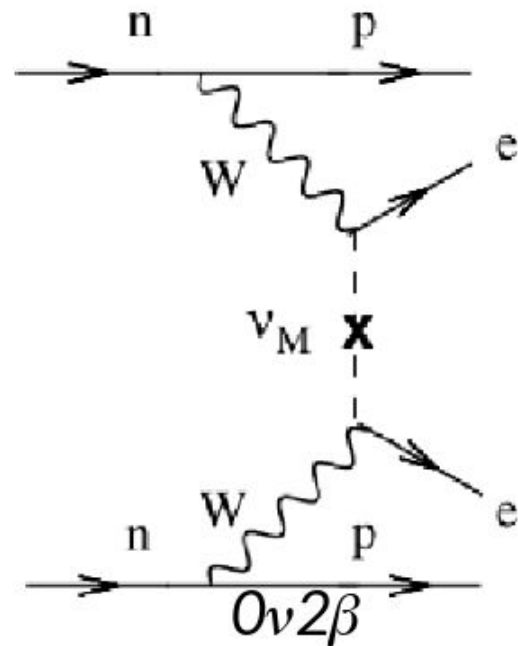
On Transition Probabilities in Double Beta-Disintegration

W. H. FURRY

Physics Research Laboratory, Harvard University, Cambridge, Massachusetts

(Received October 16, 1939)

The phenomenon of double β -disintegration is one for which there is a marked difference between the results of Majorana's symmetrical theory of the neutrino and those of the original Dirac-Fermi theory. In the older theory double β -disintegration involves the emission of four particles, two electrons (or positrons) and two antineutrinos (or neutrinos), and the probability of disintegration is extremely small. In the Majorana theory only two particles—the electrons or positrons—have to be emitted, and the transition probability is much larger. Approximate values of this probability are calculated on the Majorana theory for the various Fermi and Konopinski-Uhlenbeck expressions for the interaction energy. The selection rules are derived, and are found in all cases to allow transitions with $\Delta i = \pm 1, 0$. The results obtained with the Majorana theory indicate that it is not at all certain that double β -disintegration can never be observed. Indeed, if in this theory the interaction expression were of Konopinski-Uhlenbeck type this process would be quite likely to have a bearing on the abundances of isotopes and on the occurrence of observed long-lived radioactivities. If it is of Fermi type this could be so only if the mass difference were fairly large ($\epsilon \gtrsim 20$, $\Delta M \gtrsim 0.01$ unit).



Physicists are poor at communicating to the public!

“Search for neutrinoless double beta decay”

“Search for creation of matter”

“Search for reactions with matter/antimatter asymmetry”

Experimental Signature and current limits

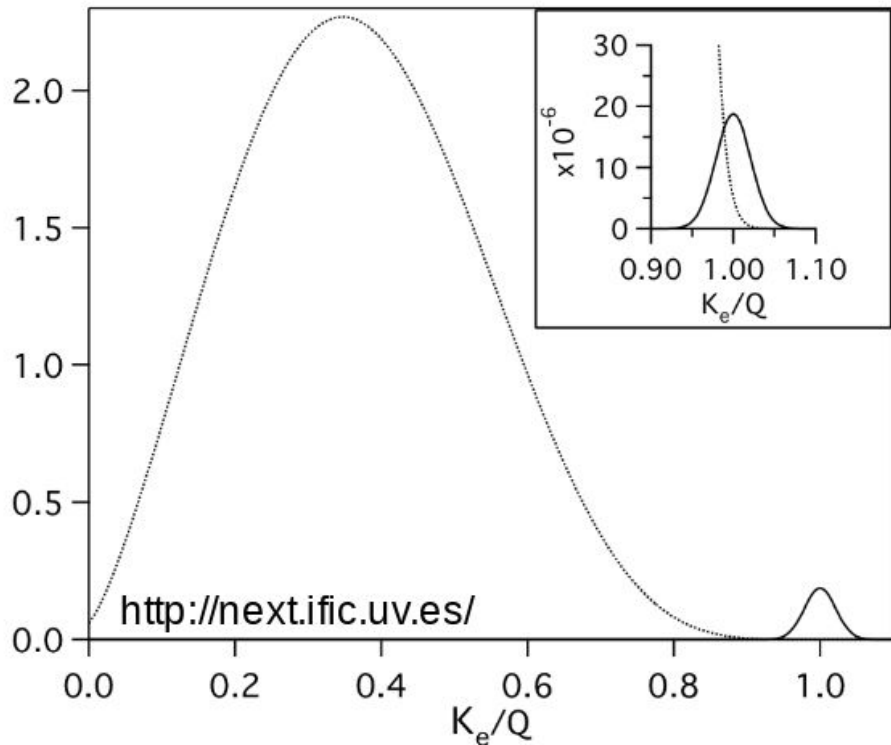


Table 2 $T_{1/2}^{0\nu}$ and $\langle m_{\beta\beta} \rangle$ limits (90% C.L.) from the most recent measurements, sorted by the mass number. The $\langle m_{\beta\beta} \rangle$ limits are listed as reported in refereed publications. Other unpublished preliminary results are described in the text.

Isotope	$T_{1/2}^{0\nu} (\times 10^{25} \text{ y})$	$\langle m_{\beta\beta} \rangle (\text{eV})$	Experiment	Reference
^{48}Ca	$> 5.8 \times 10^{-3}$	$< 3.5 - 22$	ELEGANT-IV	(157)
^{76}Ge	> 8.0	$< 0.12 - 0.26$	GERDA	(158)
	> 1.9	$< 0.24 - 0.52$	MAJORANA DEMONSTRATOR	(159)
^{82}Se	$> 3.6 \times 10^{-2}$	$< 0.89 - 2.43$	NEMO-3	(160)
^{96}Zr	$> 9.2 \times 10^{-4}$	$< 7.2 - 19.5$	NEMO-3	(161)
^{100}Mo	$> 1.1 \times 10^{-1}$	$< 0.33 - 0.62$	NEMO-3	(162)
^{116}Cd	$> 1.0 \times 10^{-2}$	$< 1.4 - 2.5$	NEMO-3	(163)
^{128}Te	$> 1.1 \times 10^{-2}$	—	—	(164)
^{130}Te	> 1.5	$< 0.11 - 0.52$	CUORE	(124)
^{136}Xe	> 10.7	$< 0.061 - 0.165$	KamLAND-Zen	(165)
	> 1.8	$< 0.15 - 0.40$	EXO-200	(166)
^{150}Nd	$> 2.0 \times 10^{-3}$	$< 1.6 - 5.3$	NEMO-3	(167)

Where we are

4

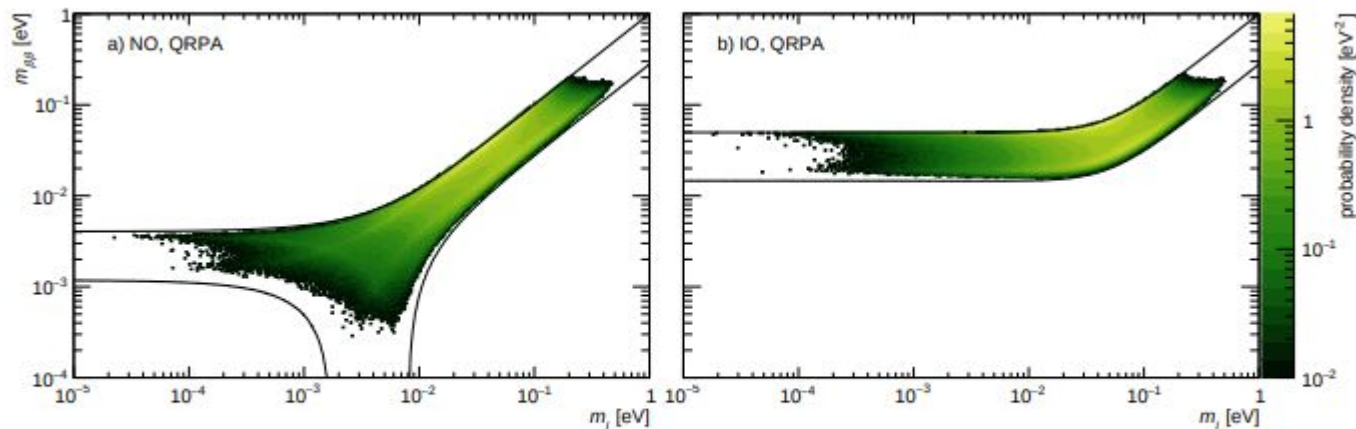


FIG. 1. Marginalized posterior distributions for $m_{\beta\beta}$ and m_l for NO (a) and IO (b). The solid lines show the allowed parameter space assuming 3σ intervals of the neutrino oscillation observables from nu-fit [12]. The plot is produced assuming QRPA NMEs and the absence of mechanisms that drive m_l or $m_{\beta\beta}$ to zero. The probability density is normalized by the logarithm of $m_{\beta\beta}$ and of m_l .

Need two orders of magnitude in effective neutrino mass=4 orders of magnitude in detector FV!

Agostini M, Benato G, Detwiler J. *Phys. Rev. D*96:053001 (2017)

Nuclear matrix elements

Largely nuclear theory required to improve things

Argues for multiple experiments with different isotopes

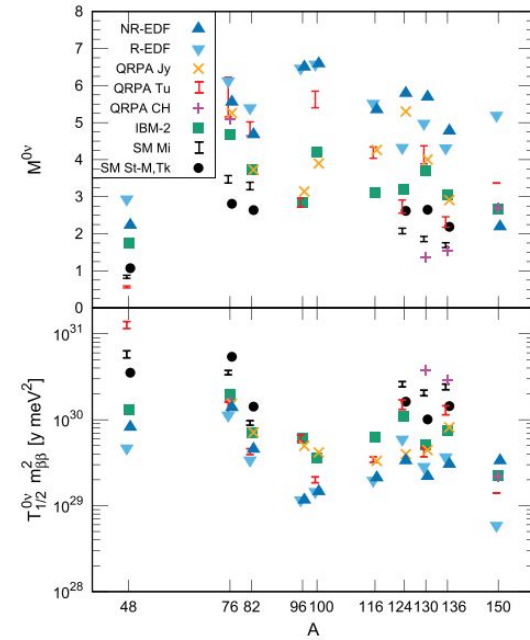
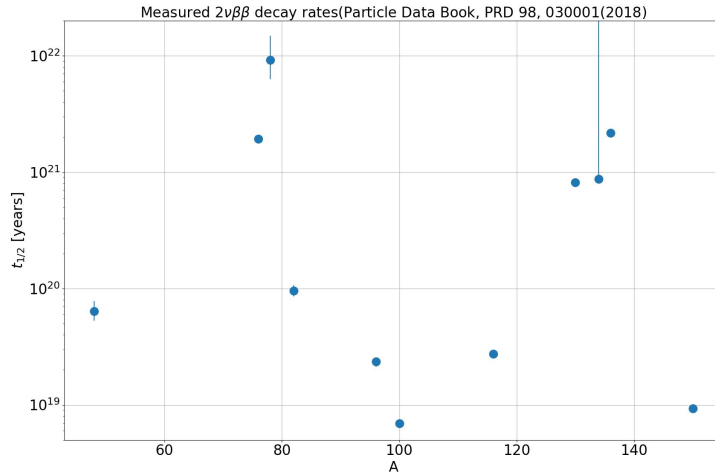


Figure 5. Top panel: nuclear matrix elements ($M^{0\nu}$) for $0\nu\beta\beta$ decay candidates as a function of mass number A . All the plotted results are obtained with the assumption that the axial coupling constant g_A is quenched and are from different nuclear models: the shell model (SM) from the Strasbourg–Madrid (black circles) [113], Tokyo (black circle in ^{48}Ca) [114], and Michigan (black bars) [82] groups; the interacting boson model (IBM-2, green squares) [109]; different versions of the quasiparticle random-phase approximation (QRPA) from the Tübingen (red bars) [115, 116], Jyväskylä (orange times signs) [81], and Chapel Hill (magenta crosses) [117] groups; and energy density functional theory (EDF), relativistic (downside cyan triangles) [118, 119] and non-relativistic (blue triangles) [120]. QRPA error bars result from the use of two realistic nuclear interactions, while shell model error bars result from the use of several different treatments of short range correlations. Bottom panel: associated $0\nu\beta\beta$ decay half-lives, scaled by the square of the unknown parameter $m_{\beta\beta}$.

NEMO-3 Tracking detector

RESULTS OF THE SEARCH FOR NEUTRINOLESS ...

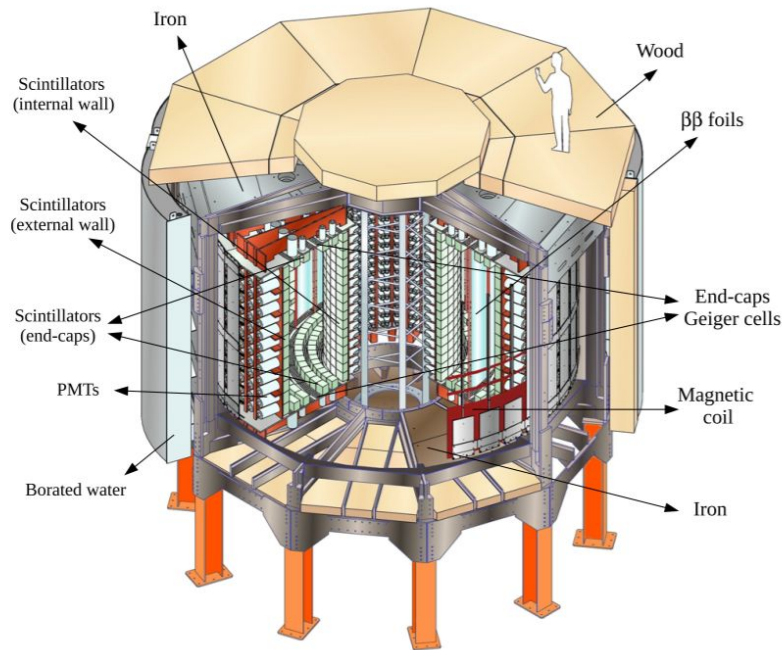


FIG. 1 (color online). A schematic view of the NEMO-3 detector, showing the double- β source foils, the tracking chamber, the calorimeter composed of scintillator blocks and PMTs, the magnetic coil and the shield.

PHYSICAL REVIEW D **92**, 072011 (2015)

Half-life measurements of the two-neutrino double- β decay

The measured half-life values for the transitions $(Z,A) \rightarrow (Z+2,A) + 2e^- + 2\bar{\nu}_e$ to the 0^+ ground state of the final nucleus are listed. We also list the transitions to an excited state of the final nucleus (0_1^+ , etc.). We report only the measurements with the smallest (or comparable) uncertainty for each transition.

$t_{1/2}(10^{21} \text{ yr})$	ISOTOPE	TRANSITION	METHOD	DOCUMENT ID
● ● ● We do not use the following data for averages, fits, limits, etc. ● ● ●				
> 0.87	^{134}Xe		EXO-200	¹ ALBERT 17c
$0.82 \pm 0.02 \pm 0.06$	^{130}Te		CUORE-0	² ALDUINO 17
$0.00690 \pm 0.00015 \pm 0.00037$	^{100}Mo		CUPID	³ ARMENGAUD 17
$0.0274 \pm 0.0004 \pm 0.0018$	^{116}Cd		NEMO-3	⁴ ARNOLD 17
$0.064 \begin{smallmatrix} +0.007 \\ -0.006 \end{smallmatrix} \begin{smallmatrix} +0.012 \\ -0.009 \end{smallmatrix}$	^{48}Ca		NEMO-3	⁵ ARNOLD 16
$0.00934 \pm 0.00022 \begin{smallmatrix} +0.00062 \\ -0.00060 \end{smallmatrix}$	^{150}Nd		NEMO-3	⁶ ARNOLD 16A
1.926 ± 0.094	^{76}Ge		GERDA	⁷ AGOSTINI 15A
0.00693 ± 0.00004	^{100}Mo		NEMO-3	⁸ ARNOLD 15
$2.165 \pm 0.016 \pm 0.059$	^{136}Xe		EXO-200	⁹ ALBERT 14
$9.2 \begin{smallmatrix} +5.5 \\ -2.6 \end{smallmatrix} \pm 1.3$	^{78}Kr		BAKSAN	¹⁰ GAVRILYAK 13
$2.38 \pm 0.02 \pm 0.14$	^{136}Xe		KamLAND-Zen	¹¹ GANDO 12A
$0.7 \pm 0.09 \pm 0.11$	^{130}Te		NEMO-3	¹² ARNOLD 11
$0.0235 \pm 0.0014 \pm 0.0016$	^{96}Zr		NEMO-3	¹³ ARGYRADES 10
$0.69 \begin{smallmatrix} +0.10 \\ -0.08 \end{smallmatrix} \pm 0.07$	^{100}Mo	$0^+ \rightarrow 0_1^+$	Ge coinc.	¹⁴ BELLI 10
$0.57 \begin{smallmatrix} +0.13 \\ -0.09 \end{smallmatrix} \pm 0.08$	^{100}Mo	$0^+ \rightarrow 0_1^+$	NEMO-3	¹⁵ ARNOLD 07
$0.096 \pm 0.003 \pm 0.010$	^{82}Se		NEMO-3	¹⁶ ARNOLD 05A
$0.029 \begin{smallmatrix} +0.004 \\ -0.003 \end{smallmatrix}$	^{116}Cd		$^{116}\text{CdWO}_4$ scint. ¹⁷	DANEVICH 03

¹ ALBERT 17c uses the EXO-200 detector that contains $19.098 \pm 0.014\%$ admixture of ^{134}Xe to search for the $2\nu\beta\beta$ decay mode. The exposure is 29.6 kg-year. The median sensitivity is 1.2×10^{21} years.

² ALDUINO 17 use the CUORE-0 detector containing 10.8 kg of ^{130}Te in 52 crystals of TeO_2 . The exposure was 9.3 kg yr of ^{130}Te . This is a more accurate rate determination than in ARNOLD 11 and BARABASH 11A.

³ ARMENGAUD 17 use 185.9 ± 0.1 g crystal of $\text{Li}_2^{100}\text{MoO}_4$ to determine the ^{100}Mo $2\nu\beta\beta$ half-life. The exposure was of 1303 ± 26 hours only, using novel technique.

Background/kg also needs to be reduced by 10000

Personal opinion: A complete and demonstrable background model is the single most important measure of the believability of a result. You want to show you understand backgrounds at all energies and all positions.

Big steps in background rejection have come from a variety of techniques, including materials selection/chemistry, processing techniques, detector innovations, and data processing/analysis/particle identification.

Large Liquid Scintillator Detectors: Kamland-Zen and SNO+

Kamland-Zen is the most sensitive experiment with half-life $> 1.07 \times 10^{26}$ y.

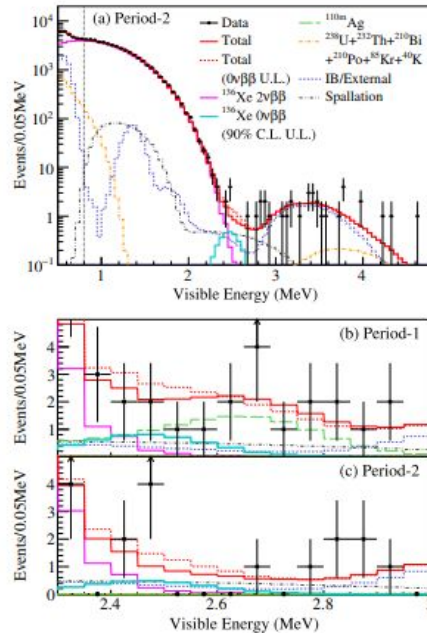


FIG. 2. (a) Energy spectrum of selected $\beta\beta$ candidates within a 1-m-radius spherical volume in period 2 drawn together with best-fit backgrounds, the $2\nu\beta\beta$ decay spectrum, and the 90% C.L. upper limit for $0\nu\beta\beta$ decay. [(b) and (c)] Close-up energy spectra for $2.3 < E < 3.0$ MeV in period 1 and period 2, respectively.

But because of my personal Connections I will concentrate on SNO+...

PRL 117, 082503 (2016)

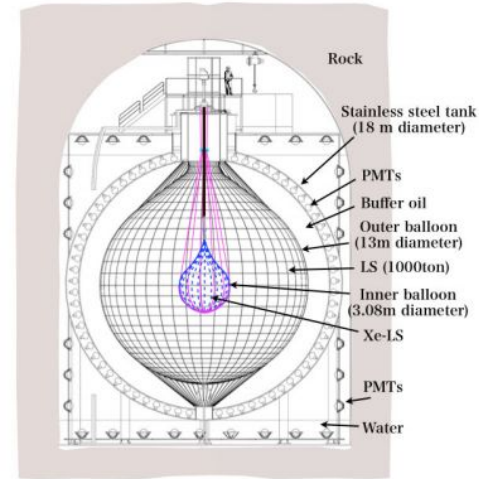


Table 2 T. by the mass Other unpu

is, sorted ications.

Isotope	Reference
^{48}Ca	(157)
^{76}Ge	(158)
^{82}Se	(159)
^{96}Zr	(160)
^{100}Mo	(161)
^{116}Cd	(162)
^{128}Te	(163)
^{130}Te	(164)
^{136}Xe	(165)
^{150}Nd	(166)

Isotope	Reference
^{48}Ca	(157)
^{76}Ge	(158)
^{82}Se	(159)
^{96}Zr	(160)
^{100}Mo	(161)
^{116}Cd	(162)
^{128}Te	(163)
^{130}Te	(164)
^{136}Xe	(165)
^{150}Nd	(166)

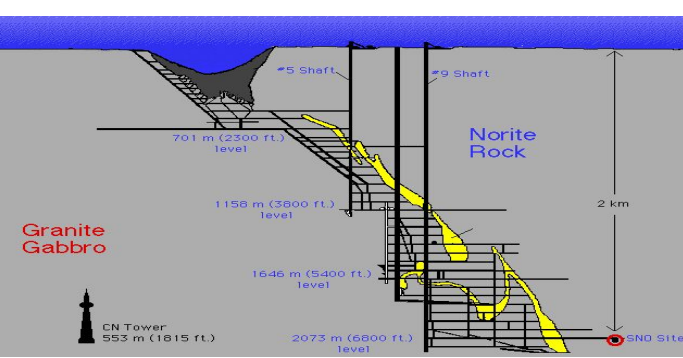
Isotope	Reference
^{48}Ca	(157)
^{76}Ge	(158)
^{82}Se	(159)
^{96}Zr	(160)
^{100}Mo	(161)
^{116}Cd	(162)
^{128}Te	(163)
^{130}Te	(164)
^{136}Xe	(165)
^{150}Nd	(166)

Isotope	Reference
^{48}Ca	(157)
^{76}Ge	(158)
^{82}Se	(159)
^{96}Zr	(160)
^{100}Mo	(161)
^{116}Cd	(162)
^{128}Te	(163)
^{130}Te	(164)
^{136}Xe	(165)
^{150}Nd	(166)

SNO+



SNO



1000 tonnes D_2O

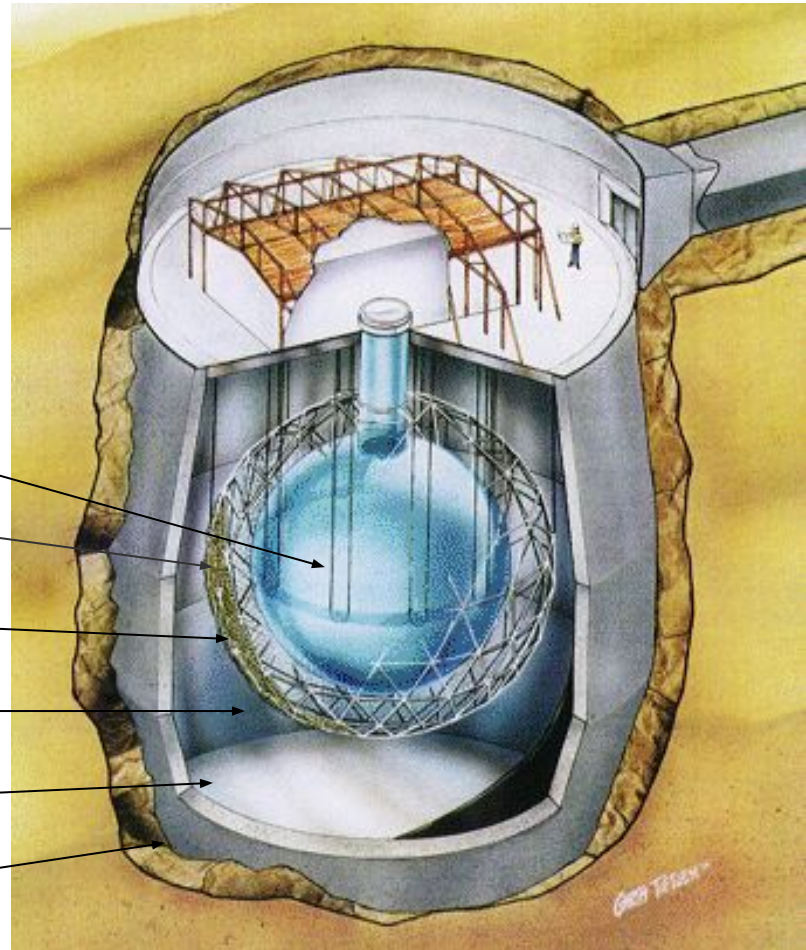
Support Structure for 9500 PMTs,
60% coverage

12 m Diameter Acrylic Vessel

1700 tonnes Inner Shielding H_2O

5300 tonnes Outer Shield H_2O

Urylon Liner and Radon Seal



Upgraded DAQ

Upgraded Electronics

New Calibration system



Cover gas system
Limit Rn ingress

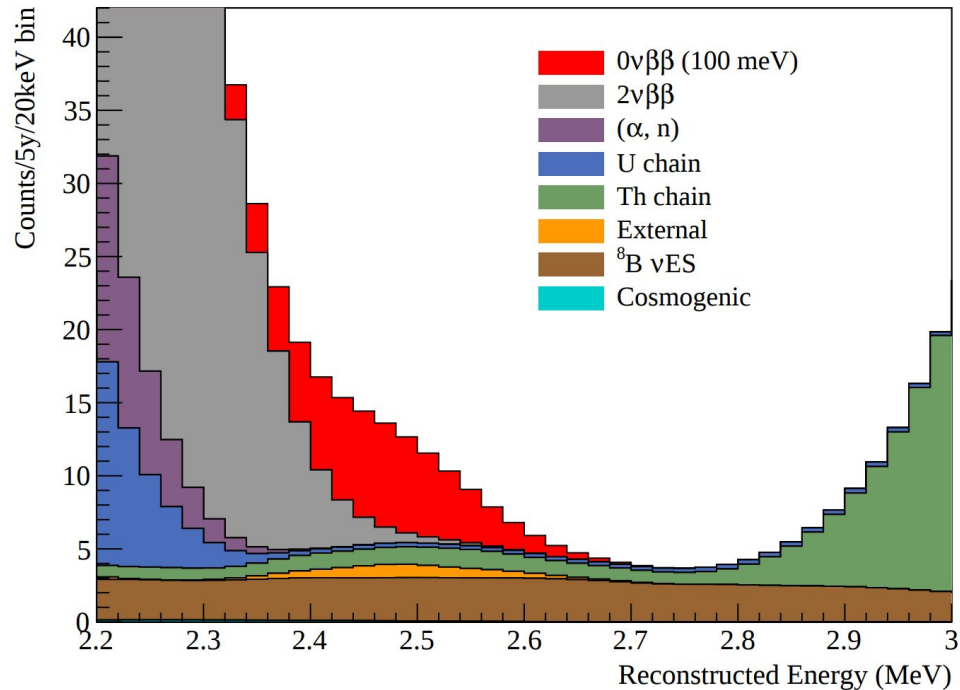
Repair Cavity Liner

New hold-down ropes system
LS lighter than water

Repaired PMTs

Underwater Cameras

SNO+ Expected Signal and Backgrounds



- Better energy resolution would obviously help
- Biggest background is ${}^8\text{B}$ solar neutrinos!
Work is ongoing to see if Cerenkov component of very prompt light can be used to suppress solar neutrinos.
- Pulse shape discrimination might be useful to suppress gammas.
- Taking advantage of large isotopic abundance (34%) of ${}^{130}\text{Te}$, small $2\nu\beta\beta$ decay rate, large ${}^{214}\text{Bi}$ - ${}^{214}\text{Po}$ rejection factor
- Very scalable:



Enriched Germanium Detectors: GERDA. Halflife $> 8 \times 10^{25}$ y.

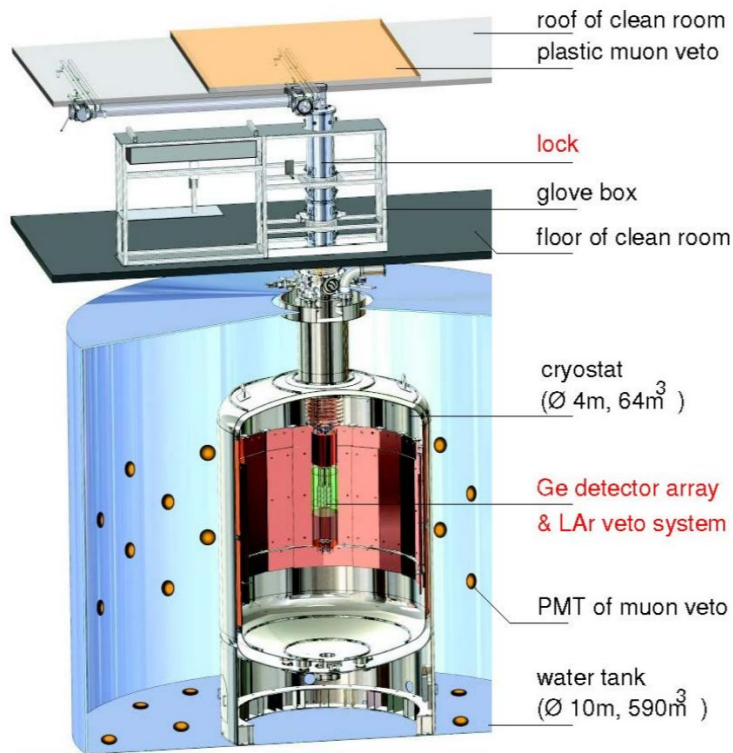


Fig. 1 GERDA setup. The new Phase II components are labeled in red.

PHYSICAL REVIEW LETTERS **120**, 132503 (2018)

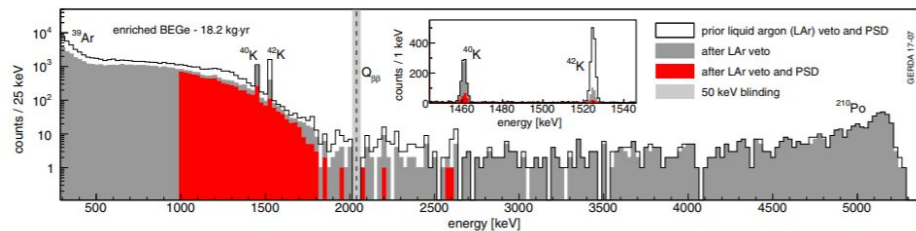


FIG. 1. Energy spectra of Phase II BEGe detectors prior to liquid argon veto and PSD cuts (total histogram), after additional LAr veto (dark gray) and after after all cuts (red). The inset shows the spectrum in the energy region of the potassium lines (1460 keV from ^{40}K and 1525 keV from ^{42}K). The gray vertical band indicates the blinded region of ± 25 keV around the $Q_{\beta\beta}$ value.

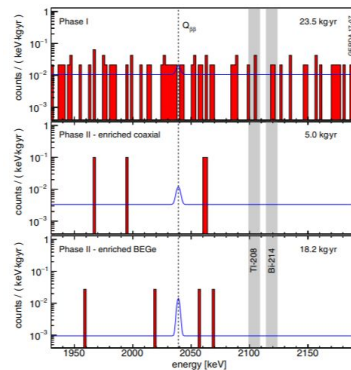


FIG. 2. Energy spectra in the analysis window for Phase I and Phase II coaxial detectors and Phase II BEGe detectors, respectively, after all cuts. The binning is 2 keV. The gray vertical bands indicate the intervals excluding known γ lines. The blue lines show the hypothetical $0\nu\beta\beta$ signal for $T_{1/2}^0 = 8.0 \times 10^{25}$ yr, on top of their respective constant backgrounds.

- Background free!
- Extremely good energy resolution (3-4 keV FWHM at 2039 keV $Q_{\beta\beta}$)
- Small electrode detectors; ability to distinguish very local energy deposits in bulk from multisite or surface events
-

Majorana Demonstrator:

PHYSICAL REVIEW LETTERS **120**, 132502 (2018)

The MAJORANA Collaboration is operating an array of high purity Ge detectors to search for neutrinoless double- β decay in ^{76}Ge . The MAJORANA DEMONSTRATOR comprises 44.1 kg of Ge detectors (29.7 kg enriched in ^{76}Ge) split between two modules contained in a low background shield at the Sanford Underground Research Facility in Lead, South Dakota. Here we present results from data taken during construction, commissioning, and the start of full operations. We achieve unprecedented energy resolution of 2.5 keV FWHM at $Q_{\beta\beta}$ and a very low background with no observed candidate events in 9.95 kg yr of enriched Ge exposure, resulting in a lower limit on the half-life of $1.9 \times 10^{25}\text{ yr}$ (90% C.L.). This result constrains the effective Majorana neutrino mass to below 240–520 meV, depending on the matrix elements used. In our experimental configuration with the lowest background, the background is $4.0_{-2.5}^{+3.1}\text{ counts}/(\text{FWHM t yr})$.

DOI: 10.1103/PhysRevLett.120.132502

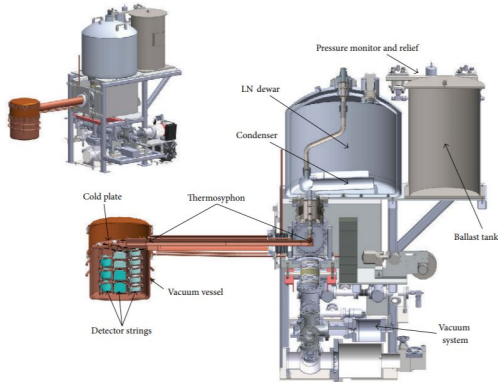


FIGURE 6: The MAJORANA DEMONSTRATOR module. Detector Strings are housed within ultralow background cryostats, each of which are supplied with its own vacuum and cryogenic systems (see text for details of vacuum and cryogenic system function).

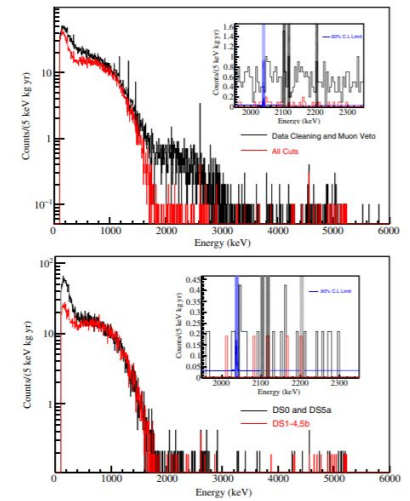


FIG. 1. Top: The spectrum above 100 keV of all six data sets summed together with only data reduction and muon veto cuts (black) and after all cuts (red). Bottom: The spectrum above 100 keV after all cuts from the higher background data sets DS0 and DSSa (black) compared to the data sets with lower background, DS1-4,5b (red). Note the γ background in DS0 is higher and the α rate is the same without pulse shape analysis. Rejection of α particles in DSSa is degraded due to noise as described in the text. Insets: The same as in the primary plots but for the 360-keV region. The blue and graded shaded regions are excluded when determining the background. The thin blue curves shows the 90% C.L. upper limit for $0\nu\beta\beta$ at $Q_{\beta\beta}$ as described in the text, which corresponds to 2.04 signal counts.

- Background free
- 2.5 keV resolution
- Point contact detectors
- Has joined with Gerda->LEGEND

EXO-200 ^{136}Xe TPC

Results from a search for neutrinoless double-beta decay ($0\nu\beta\beta$) of ^{136}Xe are presented using the first year of data taken with the upgraded EXO-200 detector. Relative to previous searches by EXO-200, the energy resolution of the detector has been improved to $\sigma/E = 1.23\%$, the electric field in the drift region has been raised by 50%, and a system to suppress radon in the volume between the cryostat and lead shielding has been implemented. In addition, analysis techniques that improve topological discrimination between $0\nu\beta\beta$ and background events have been developed. Incorporating these hardware and analysis improvements, the median 90% confidence level $0\nu\beta\beta$ half-life sensitivity after combining with the full data set acquired before the upgrade has increased twofold to 3.7×10^{25} yr. No statistically significant evidence for $0\nu\beta\beta$ is observed, leading to a lower limit on the $0\nu\beta\beta$ half-life of 1.8×10^{25} yr at the 90% confidence level.

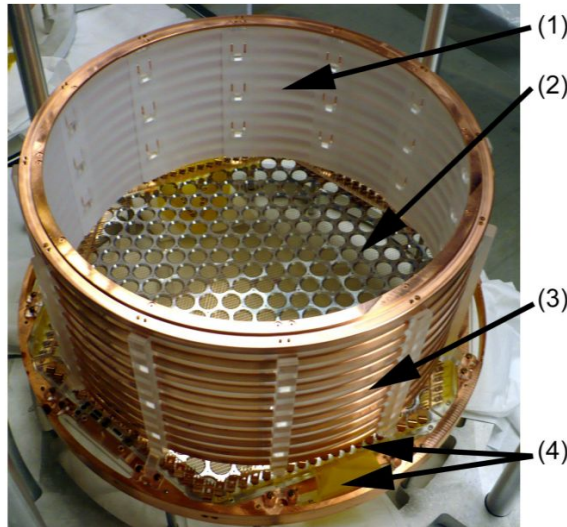


Figure 4. A view into the active Xe volume of one of the two EXO-200 TPC modules. PTFE tiles (1) installed inside the field-shaping rings serve as reflectors for the scintillation light. The aluminum-coated side of the LAAPD platter (2) is visible, as well as the field cage (3), ionization wires, and flexible cables (4).

JINST 7 P05010 (2012)

PHYSICAL REVIEW LETTERS 120, 072701 (2018)

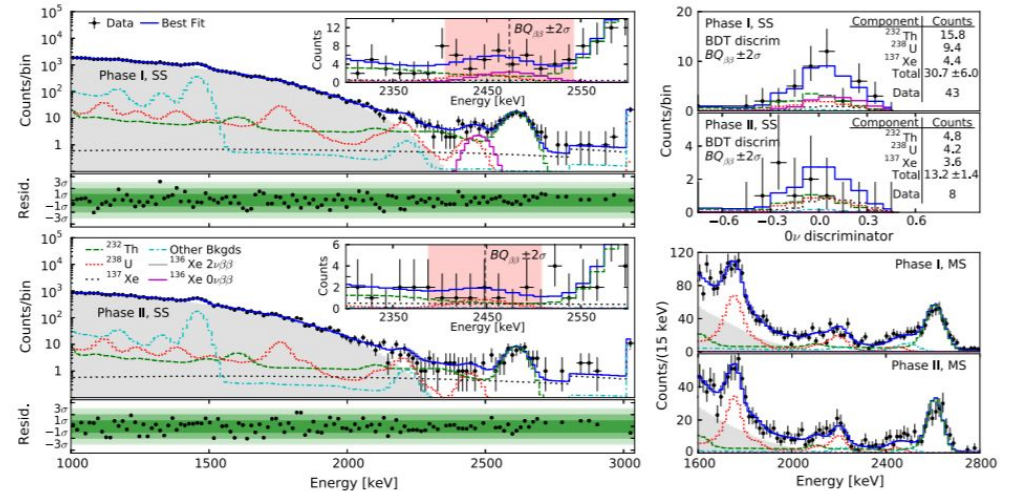


FIG. 4. Best fit to the low-background data SS energy spectrum for Phase I (top left) and Phase II (bottom left). The energy bins are 15 and 30 keV below and above 2800 keV, respectively. The inset shows a zoomed-in view around the best-fit value for $BQ_{\beta\beta}$. Top right: Projection of events within $BQ_{\beta\beta} \pm 2\sigma$ on the BDT fit dimension. Bottom right: MS energy spectra above the ^{40}K γ line.

CUORE: Cryogenic Bolometer

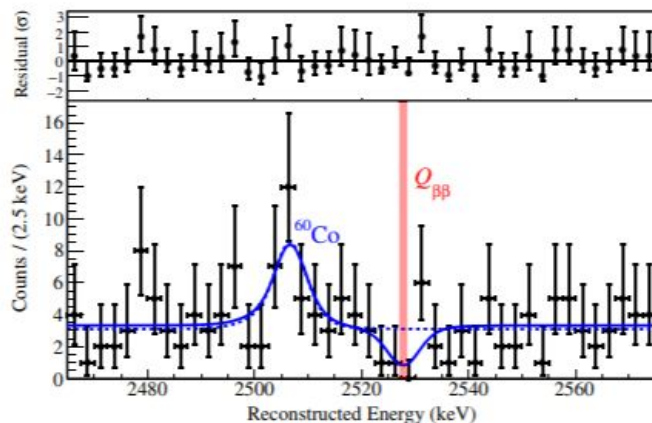
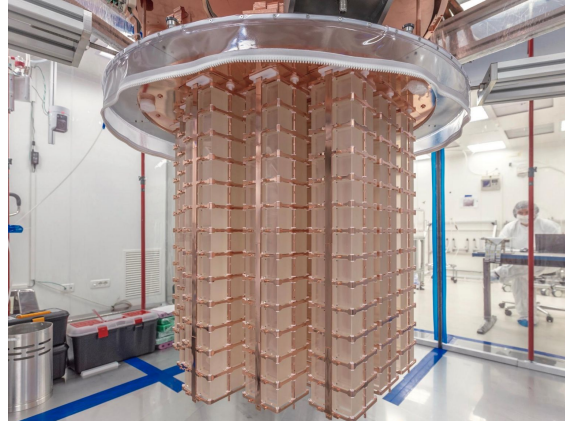


FIG. 3. Bottom: Best-fit model from the UEMF fit (solid blue line) overlaid on the spectrum of $0\nu\beta\beta$ decay candidates observed in CUORE. The peak near 2506 keV is attributed to ^{60}Co [33]. The normalized residuals of this model and the binned data are shown in the top panel. The dashed (blue) curve shows the best fit for a model with no $0\nu\beta\beta$ decay component. The vertical band is centered at $Q_{\beta\beta}$; the width of the band reflects the systematic uncertainty on the reconstructed energy.

PHYSICAL REVIEW LETTERS **120**, 132501 (2018)

The CUORE experiment, a ton-scale cryogenic bolometer array, recently began operation at the Laboratori Nazionali del Gran Sasso in Italy. The array represents a significant advancement in this technology, and in this work we apply it for the first time to a high-sensitivity search for a lepton-number-violating process: ^{130}Te neutrinoless double-beta decay. Examining a total TeO_2 exposure of 86.3 kg yr, characterized by an effective energy resolution of (7.7 ± 0.5) keV FWHM and a background in the region of interest of (0.014 ± 0.002) counts/(keV kg yr), we find no evidence for neutrinoless double-beta decay. Including systematic uncertainties, we place a lower limit on the decay half-life of $T_{1/2}^{0\nu}(^{130}\text{Te}) > 1.3 \times 10^{25}$ yr (90% C.L.); the median statistical sensitivity of this search is 7.0×10^{24} yr. Combining this result with those of two earlier experiments, Cuoricino and CUORE-0, we find $T_{1/2}^{0\nu}(^{130}\text{Te}) > 1.5 \times 10^{25}$ yr (90% C.L.), which is the most stringent limit to date on this decay. Interpreting this result as a limit on the effective Majorana neutrino mass, we find $m_{\beta\beta} < (110 - 520)$ meV, where the range reflects the nuclear matrix element estimates employed.

DOI: [10.1103/PhysRevLett.120.132501](https://doi.org/10.1103/PhysRevLett.120.132501)

Summary

Finding Neutrinoless Double Beta Decay is compelling physics and a high priority.

We need to expect that detectors might need to scale in size and purity by 3-4 orders of magnitude.

There is an active and ingenious international program developing a variety of technologies in a variety of isotopes. I have only shown a sample.